

Manuscript Number: CERI-D-16-07965R2

Title: SOLUTION COMBUSTION SYNTHESIS OF (Co,Ni)Cr₂O₄ PIGMENTS: INFLUENCE OF INITIAL SOLUTION CONCENTRATION

Article Type: Full length article

Keywords: Powders: chemical preparation (A); colour (C); spinels (D); solution concentration

Corresponding Author: Mrs. Jessica Gilabert, M.Sc.

Corresponding Author's Institution: Instituto de Tecnología Cerámica (ITC). Asociación de Investigación de las Industrias Cerámicas (AICE)

First Author: Jessica Gilabert, M.Sc.

Order of Authors: Jessica Gilabert, M.Sc.; Maria Dolores Palacios, PhD; Vicente Sanz, PhD; Sergio Mestre, PhD

Abstract: Initial solution concentration effect was studied on the synthesis of mixed spinels Co₁-YNiYCr₂O₄ (0 ≤ Y ≤ 1) obtained by Solution Combustion Synthesis. Fd-3m spinel structure was developed in all range of compositions analysed, regardless of the concentration. However, structural characteristics such as ion rearrangement and crystal size showed a noticeable dependence on the initial concentration, being the spinel network more ordered and with higher crystallite size as the concentration increased. Cell parameter, however, presented dependence on composition but not on initial solution concentration.

All as-synthesized pigments showed a significant colouring power in ceramic glazes without any significant influence of initial solution concentration. Therefore, a second thermal treatment was not needed. The coloured glazes covered a broad range of tones in the green section of colour space, which evolved as a function of composition.

SOLUTION COMBUSTION SYNTHESIS OF (Co,Ni)Cr₂O₄

PIGMENTS: INFLUENCE OF INITIAL SOLUTION CONCENTRATION

J. Gilabert^{a,*}, M.D. Palacios^b, V. Sanz^{b,c}, S. Mestre^{b,c}

^aInstituto de Tecnología Cerámica. Asociación de Investigación de las Industrias Cerámicas.

Castellón (Spain)

^bInstituto Universitario de Tecnología Cerámica. Universitat Jaume I. Castellón (Spain)

^cDepartamento de Ingeniería Química. Universitat Jaume I. Castellón (Spain)

*Corresponding Author (jessica.gilabert@itc.uji.es)

Abstract

Initial solution concentration effect was studied on the synthesis of mixed spinels Co_{1- Ψ} Ni _{Ψ} Cr₂O₄ (0 $\leq\Psi\leq$ 1) obtained by Solution Combustion Synthesis. Fd-3m spinel structure was developed in all range of compositions analysed, regardless of the concentration. However, structural characteristics such as **ion rearrangement** and crystal size showed a noticeable dependence on the initial concentration, being the **spinel network more ordered** and with higher crystallite size as the concentration increased. Cell parameter, however, presented dependence on composition but not on initial solution concentration.

All as-synthesized pigments showed a significant colouring power in ceramic glazes without any significant influence of initial solution concentration. Therefore, a second thermal treatment was not needed. The coloured glazes covered a broad range of tones in the green section of colour space, which evolved as a function of composition.

Keywords: Powders: chemical preparation (A); colour (C); spinels (D); solution concentration

1 Introduction

Submicronic materials with characteristic structural dimensions have been of interest for more than 20 years and continue to attract attention because of their unique properties [1]. Such materials have found a variety of applications in different branches of industry including microtechnology, biotechnology and surface coatings, as well as energy storage and conversion devices, such as fuel cells.

In the case of the traditional ceramic sector, submicronic powders are greatly welcomed when inkjet technology is wanted to be applied. Nanosized ceramic pigments are needed in order to develop a good quality inks, which are able to pass through the printer nozzles without damaging the mechanical system. At the same time, pigments must be able to develop intense colours. These inks are currently manufactured by micronizing conventional ceramic pigments down to average diameters of 0.2-0.6 μm [2]. To prevent print head nozzles from clogging, the most important requirement is to ensure that 99% of the pigment particles are less than 1 μm in diameter [3,4]. This fact demands a very different approach to the comminution stage: from controlling average particle size during jet milling (conventional pigments) to ensure that practically all particles are submicronic.

A wide variety of techniques are used to obtain materials at microscale in industry. The most basic one used in ceramic sector is high-energy milling. However, this process is energy intensive and frequently consumes spare parts of the mill, resulting in high costs. Furthermore, this milling process presents the drawback of damaging ceramic pigment's crystalline structure and, as a consequence, their tinting strength is reduced [5]. All these inconvenient have encouraged companies and research centres to foster in the development of innovative synthetic routes with a lower cost of production of nanopigments with the optimum structure.

An alternative methodology that has stood out because of its capability for obtaining fine particles is the so-called solution combustion synthesis (SCS). This method is a combination of combustion and a reactive solution approach. SCS involves a self-sustained reaction in a

1 solution of metal nitrates and different fuels as urea or glycine. The reaction between fuel and
2 oxygen-containing species formed during decomposition of nitrates provides conditions for
3 rapid high-temperature interaction [6]. The initial liquid solution of nitrate precursors, after fast
4 preheating to moderate temperatures (500°C) self-ignites over the whole volume (volume
5 solution combustion mode (VSC)) leading to the formation of a very spongy mass with tailored
6 composition.
7

8
9
10
11
12
13 SCS was reported to be a technology able to synthesize simple and complex oxides used as
14 pigments or advanced ceramics [7-9]. It contributes to nanopigment development with special
15 features [10-13] because of its characteristic combustion process. On one hand, the reactant
16 mixing is really effective since starting media is an aqueous solution, which favours cations to
17 be mixed on a molecular scale. On the other hand, under the appropriate conditions the high
18 temperatures (~1500°C) reached in the solution combustion synthesis method allow obtaining
19 oxide products, as ceramic pigments are, with a high purity and good crystallinity [6]. Finally,
20 as the whole combustion process is carried out in a few minutes (short reaction time), with the
21 release of secondary products as a high volume of gases, there is an inhibition of particle size
22 growth and a spongy microstructure development. These facts contribute to obtain a solid
23 product with a very low bulk density, easy to mill.
24
25
26
27
28
29
30
31
32
33
34
35
36
37
38

39 Despite all advantages that SCS technology provides, the published studies are mainly focused
40 on characterizing synthesized products and practically no information is available about the
41 effect of modifying the process variables like selected fuel, initial solution concentration or
42 maximum temperature. Therefore, the aim of this study is centred on evaluating the effect of the
43 initial solution concentration over the synthesis of pigments $\text{Co}_{1-\psi}\text{Ni}_{\psi}\text{Cr}_2\text{O}_4$ carried out by
44 means of solution combustion synthesis. The solid solutions between spinels CoCr_2O_4 and
45 NiCr_2O_4 were selected as a result of being two of the most frequently pigments used in the
46 ceramic industry, according to the Color Pigments Manufacturer Association (CPMA) [14]. The
47 study is also intended to evaluate whether the final pigments are chemically and thermally stable
48 against the ceramic glaze once applied.
49
50
51
52
53
54
55
56
57
58
59
60
61
62
63
64
65

2 Material and methods

1
2
3 $\text{Co}_{1-\Psi}\text{Ni}_{\Psi}\text{Cr}_2\text{O}_4$ ($0 \leq \Psi \leq 1$, in steps of 0.2) pigments were synthesized from their corresponding
4
5 **Co, Ni and Cr nitrates mixed with urea as fuel and water as a solvent** (All reactants used were
6
7 from Panreac Química, S.A.U. Spain). Urea proportion was calculated following the reaction
8
9 stoichiometry in order to reach the combustion of the whole mixture. Table I shows the initial
10
11 solutions' compositions. The proportion of water was changed in order to study the initial
12
13 solution concentration effect in the synthesis of the pigments. Consequently, three complete
14
15 series with different initial solution concentration of spinel precursors were prepared: 2.4 M, 1.2
16
17 M and 0.6 M, which from now on will be referenced as high, medium and low solution
18
19 concentration, respectively.
20
21
22
23

24
25 The first aim was to maintain the volume of solution in each experiment constant, in order to
26
27 avoid increasing the number of variables to be taken into account. However, due to the high
28
29 volume of the combustion product obtained in some experiments, it was necessary to readjust
30
31 the original solution volume so as to avoid any contamination of the kiln chamber and their
32
33 refractories.
34
35

36
37 All solutions were poured in a 700-mL pyrex container of 14 cm in diameter which was inserted
38
39 in a preheated kiln at 500 °C (BLF 1800, Carbolite Furnaces Ltd, UK) during 20 min of soaking
40
41 time. **Then, the kiln was turned off and the as-synthesized pigment was progressively cooled**
42
43 **down to ambient temperature.**
44

45
46 Every pigment was wet milled to break the agglomerates in a ball mill using water as a fluid and
47
48 agate jars (Pulverisette 5, Fritsch GmbH, Germany). Afterwards, the pigments were dried under
49
50 infrared lights and sieved with a 200- μm mesh.
51

52
53 Pigments were characterized from a chemical, microstructural, mineralogical, physical and
54
55 colourimetric point of view. Chemical composition was determined by an energy-dispersive X-
56
57 ray microanalysis instrument **(EDX)** (Genesis 7000 SUTW, EDAX, USA) coupled to a **FEG-**
58
59 **SEM (Field Emission Guns-Scanning electron microscope)** (QUANTA 200F, FEI Co, USA)
60
61
62
63
64
65

1 with which the microstructural characterisation was carried out. Adsorption/desorption
2 isotherms and specific surface area values were determined according to the BET method
3
4 (Brunauer-Emmet-Teller) using nitrogen gas as adsorbate (Tristar 3000, Micromeritics, USA).
5
6 Additionally, pore size distribution was obtained from the adsorption isotherms using the
7
8 Barrett-Joyner-Halenda method (BJH).
9

10
11 Identification of crystalline phases and the posterior measurement of crystallite size and cell
12 parameters evaluation were carried out by XRD (Theta-Theta D8 Advance, Bruker, Germany),
13 with CuK radiation ($\lambda = 1.54183 \text{ \AA}$). The generator applied an intensity light source of 45 kV
14 and 40 mA. XRD data were collected in a 2θ from 5 to 90° with a step width of 0.015° and a
15 counting time of 1.2 s/step by means of a VANTEC-1 detector. Raw data were refined by
16 Rietveld method using 4.2 version of the Rietveld analysis program DIFFRACplus TOPAS. A
17 pseudo-Voigt function to describe peak shapes was assumed. The refinement protocol included
18 the background, the scale factors and the global-instrument, lattice, profile and texture
19 parameters.
20
21
22
23
24
25
26
27
28
29
30

31 To evaluate colour development, pigments were mixed in a proportion 2/98 wt% into a
32 transparent single-fired porous tile glaze (chemical composition: 0.5% Na₂O 4.0 % K₂O, 15.3%
33 CaO, 0.9 MgO, 9.0% ZnO, 7.4% Al₂O₃, 3.0% B₂O₃, 59.5% SiO₂) and fired in an electric
34 laboratory kiln according to a thermal cycle of single-fired floor tiles (maximum temperature
35 1100 °C and 6 min of soaking time). Spectrophotometric curves of the glazed tiles were
36 obtained (Color Eye 7000A, X-Rite Inc, USA), and CIELab* chromatic coordinates were
37 calculated using CIE Illuminant D65 and CIE 10° standard observer.
38
39
40
41
42
43
44
45
46
47
48

49 **3 Results and discussion**

50
51 As-obtained pigments presented a highly fluffy texture, filling the whole synthesis glass
52 container. Bulk density was quite low which made them easy to disaggregate with a low effort.
53
54 Pigment colours presented an evolution around the green tones, from a bluish green to a greyish
55 green.
56
57
58
59
60
61
62
63
64
65

3.1 Chemical composition

EDX analysis of some of the synthesized pigments showed a good correlation with theoretical values according to the initial solution compositions (Fig. 1). When pure spinels were synthesized ($\Psi=0.0$ and $\Psi=1.0$) the differences among values were smaller than in solid solution spinels. However, it has to be taken into account that EDX method is semiquantitative and little oscillations around the exact value can be produced in some samples due to the lack of planarity of the spongy samples. This latter phenomenon is responsible for modifying the signal received by EDX detectors in order to determine the molar content. The lack of planarity of the samples affects particularly the oxygen percentage determination. In previous reports published about solid solutions of spinels, a good correlation between experimental and theoretical composition was demonstrated in all Ψ range [15]. For that reason, not all pigments developed in this study have been analysed by EDX, only the most representative pigments in this case. According to obtained results, from a chemical point of view, SCS method allows obtaining homogeneous solid solutions of spinels with molar compositions practically adjusted to the theoretical ones.

3.2 Crystalline structures

Diffraction patterns showed that the main crystalline phase obtained in all the range of compositions was of spinel type, concretely the Fd-3m class (face-centred structure) [16]. However, as Ni^{2+} content increased in the composition ($\Psi > 0.0$), a rise in the proportion of a secondary phase with eskolaite structure (Cr_2O_3) [17] was also observed in the samples. Fig. 2 shows the complete diffraction patterns for all composition range of $(\text{Co,Ni})\text{Cr}_2\text{O}_4$ samples with both crystalline structures (spinel and eskolaite) identified by XRD at 1.2M concentration. According to Rietveld data, the eskolaite increasing effect was more pronounced when the solution concentration decreased (Fig. 3). This phenomenon pointed out that not all the trivalent ions were integrated into the spinel structure, although the percentage of eskolaite was not higher than a 5% in any case. Despite this circumstance, it was possible to consider that SCS

1
2
3
4
5
6
7
8
9
10
11
12
13
14
15
16
17
18
19
20
21
22
23
24
25
26
27
28
29
30
31
32
33
34
35
36
37
38
39
40
41
42
43
44
45
46
47
48
49
50
51
52
53
54
55
56
57
58
59
60
61
62
63
64
65

technique is suitable for synthesizing spinel pigments because spinel-type industrial ceramic pigments frequently contain low proportions of unreacted oxides.

On the other side, all synthesized pigments presented a high crystallinity, higher than $98 \pm 4\%$ according to Rietveld analysis. Practically no amorphous phase was observed in the samples. Nevertheless, spinel structure evolution in the solid solutions indicated the presence of an improvement in ion rearrangement to obtain a more defined structure, reaching a maximum for the spinel with $\Psi=0.8$ (Fig. 4). This phenomenon was deduced after observing that spinel main peak evolved towards higher heights and narrower and more defined shapes. Such behaviour suggested that the progressive enrichment with Ni^{2+} ion improved the capacity of obtaining a more ordered spinel structure. On the other hand, the absence of Co^{2+} provokes an obvious negative effect on spinel structure development because, as Ψ increases, a trend to increase eskolaite phase percentage at the cost of spinel formation was also observed.

Regarding the initial solution concentration, an important effect was detected based on the progression of the main peak intensity of the diffraction patterns because, as the initial solution concentration increases, the intensity peak becomes higher and more defined, indicating the rearrangement of a more ordered spinel structure. In Fig. 4 diffraction patterns of the pigments synthesized with the most concentrated solutions showed the highest peaks, which meant a better capability to obtain a more ordered structure. Such behaviour can be interpreted considering that as the solution concentrates, the volume of liquid in the synthesizing container is reduced. This phenomenon yields a faster heat transfer, which evaporates water in shorter times, limiting the possibility of ion segregation in the drying mixture and improving reactant contact during the combustion process. It can be supposed that as the concentration increases, the bulk density of the dry mixture of reactants is higher, so the energy generated by the reaction allows process to reach higher temperatures, which facilitates ions mobility and their rearrangement as spinel network.

Taking into account Fig. 3 and 4, it is possible that a relation between obtaining a more ordered structure and the eskolaite proportion exists. It could be related to different effects taking place

1 during the synthesis. On one hand, it would be possible that some chromium could not be able
2 to join the spinel structure. Therefore, the chromium positions would either be filled by other
3 ions, such as Co^{3+} or be left as a vacant. On the other hand, due to the important effect of the
4 fluorescence in the diffraction pattern of the pigments, it could be possible that some Co and Ni
5 compounds (oxides or hydroxides) were also present in the samples, but in proportions under the
6 detection limit of XRD [18-21]. Consequently, the molar relation Co/Ni versus Cr was
7 maintained in the spinel, although the network order was not favoured. To distinguish between
8 both effects, it would be necessary the use of analytical techniques, capable of detecting
9 crystalline phases in very low proportions.

10 The crystallite size was calculated in each one of the pigments (Fig. 5). The data showed a
11 progressive decrease of crystallite size as the cobalt content was reduced (from $\Psi=0$ to $\Psi=0.8$).
12 However, the absence of cobalt ($\Psi=1$) changed the global trend and crystallite size sharply
13 plummeted, up to practically a half the previous data points. The cobalt enrichment in the
14 structure seemed to favour the growth of the formed crystallite, whereas the Ni^{2+} ion exerted the
15 opposite effect.

16 Molar concentration also influences crystallite size evolution since the most concentrated
17 solution generates pigments with bigger crystallites than the diluted ones. This result agrees
18 with the proposed hypothesis about the effects of thermal treatment based on X-ray diffraction
19 patterns. According to which, it was interpreted that a higher solution concentration limits the
20 possibility of ion segregation and, at the same time, improves reactant contact during
21 combustion process, favouring ion rearrangement as spinel network.

22 No clear trend was observed in lattice parameter data against initial solution concentration (Fig.
23 6). As expected, the lattice parameter showed a clear relation with composition, as predicted by
24 Vegard's law. Theoretical lattice parameters evolved from 8.340 Å for CoCr_2O_4 spinel [22] to
25 8.315 Å for NiCr_2O_4 spinel [23]. However, a positive deviation from the theoretical line was
26 observed. In fact, experimental values presented a curved shape in which a positive deviation
27 from theoretical values is observed in $\Psi < 0.8$, but in $\Psi = 1$, the trend inverted, being the

1 theoretical values higher than the obtained ones. Deviations from theoretical path were
2 previously described in some works by Mestre et al. [9], Shou-Yong et al. [24] and Nlebedim et
3 al. [25], but no explanation has been proposed.
4
5

6
7 The general trend of lattice parameters of the cell was consistent with the lower ionic radius of
8 the Ni^{2+} (0.49 Å) with respect to the Co^{2+} (0.56 Å) in tetrahedral coordination [26]. The lower
9 the ion size is, the shorter the distance between ions becomes and, therefore, the lattice
10 parameter decreases since dimensions of the spinel cell are reduced [15].
11
12
13
14
15

16 **3.3 Morphological characterisation**

17
18 The study of morphology and grain size was carried out over the as-synthesized samples, prior
19 to the wet-milling process, since in previous studies some modifications in the composition and
20 structure were observed due to the hydration of certain non-perfectly reacted phases [15].
21
22
23
24
25

26
27 Obtained micrographies demonstrated the development of round-shaped grains in all samples
28 (Fig. 7), regardless of the composition and solution concentration. In NiCr_2O_4 spinels case
29 ($\Psi=1$) grains were near spherical, whereas a cobalt enrichment promoted more angular grains
30 with a geometry more similar to theoretical crystalline habit of spinel [27].
31
32
33
34
35
36

37 Molar concentration exerted a significant influence in grain development since in all the
38 compositions tested an increase in concentration favoured a grain growth in different degrees.
39

40 The effect observed was similar to the effect over the crystallite size, but not equal. It can be
41 assumed that an improvement in ion homogeneity, thanks to higher solution concentration,
42 agrees with the fact that both the crystallite and, consequently, the grain experienced a growth
43 [28]. Besides the general growth observed, it has to be highlighted the specific case of $\Psi=0.6$,
44 where a singular phenomenon is produced. The grain size difference between the product of the
45 diluted solution and the product of the concentrated one is the highest in comparison to rest of
46 the samples. Grains in the pigment obtained from the concentrated solution with $\Psi=0.6$ grew in
47 a considerable way, acquiring a shape that practically reflects the theoretical crystalline habit of
48 spinel. These grains are pretty angular and their faces fitted together perfectly, reducing the
49
50
51
52
53
54
55
56
57
58
59
60
61
62
63
64
65

1 intragrain porosity of the system. By contrast, the grain size of the sample obtained with $\Psi=0.8$
2 and 2.4 M (the highest crystallite size), only shows a grain size slightly higher than the sample
3 with $\Psi=1.0$. This fact demonstrates that grain and crystallite sizes are not influenced in the same
4 way by composition and concentration.
5
6

7
8
9 Specific surface data of the pigments showed lower values when initial solutions were more
10 concentrated, which totally corroborates the behaviour observed in scanning electron
11 microscopy analysis (SEM). The samples with most ordered structure presented less
12 intergranular porosity and, consequently, lower specific surface area. At the light of the results
13 (Table 2), it can be certainly said that all analysed samples exhibited well-sintered grains since
14 all specific surface values evolved in a narrow range unlike the observed values in previous
15 works in which they can reach values up to 200 m²/g in CoAl₂O₄ spinels [9, 15]. In addition,
16 although in a subtle way, the absence of Ni²⁺ in the composition improved sintering because
17 specific surface area reduced slightly.
18
19

20 To study the porosity of pigments, BJH curves were calculated from the analysis carried out on
21 isothermal curves (Fig. 8). No significant differences were observed among obtained curves.
22 Nevertheless, mention can be made of the fact that the presence of certain small-size porosity (<
23 10 nm) in the pigments obtained from 0.6M solutions could be responsible for the subtle
24 increase observed in specific surface area.
25
26
27
28
29
30
31
32
33
34
35
36
37
38
39
40
41

42 3.4 Colouring power

43 All synthesized pigments presented a high colouring power in the selected glaze. No defects
44 were observed on the surfaces like pinholes or colour heterogeneities. These facts are indicative
45 of a good integration of the pigments into the ceramic glaze, without any unfavourable
46 interaction. This behaviour is of relevant importance in order to determine the stability degree
47 of ceramic pigments synthesized by SCS.
48
49
50
51
52
53
54
55
56

57 Final glazes covered a broad colour palette in the green sector of colour space evolving with the
58 composition, from a blue-green tone to a greyish-green. The spectrophotometric curves (Fig. 9)
59
60
61
62
63
64
65

1 showed a progressive variation as the pigments enriched in Ni²⁺, which can be related with the
2 absorption bands corresponding to electron transitions of Co²⁺, Ni²⁺ and Cr³⁺ ions located in
3 spinel crystals [29, 30]. In fact, as Ψ increased, the reflectance band characteristic for blue
4 colour was reduced ($350 < \lambda < 450$ nm), which was promoted by the gradual elimination of Co²⁺
5 [31]. Red reflectance band ($\lambda > 700$ nm) also evolved negatively as Ψ increased. On the other
6 hand, the yellow reflectance band ($550 < \lambda < 680$ nm) was strengthened because of the Ni²⁺
7 content increase. All these changes generated less bluish colours with higher green components.
8 The CIELab* coordinates, increased progressively with Ψ but with different trends. L*
9 coordinate experienced a 10 units' increase, indicative of the development of brighter colours as
10 the proportion of Ni²⁺ was higher (Fig. 10 a). b* coordinate showed the gradual elimination of
11 blue component and, as a consequence, the evolution towards colours with yellow component
12 (Fig. 10 b). The range of variation in this case was the highest, practically 20 points, which was
13 a significant change in this coordinate. Nevertheless, the coordinate that seemed to experience
14 the smallest change regarding its evolution with Ni²⁺ was a* coordinate (Fig. 10 c). Its evolution
15 showed a low-defined minimum for $\Psi=0.2$, and the green component reduces progressively as
16 the proportion of Ni²⁺ increases. When $\Psi=1.0$, a significant change is produced, due to the
17 complete elimination of cobalt, which resulted in a sharp decrease in green component. Such
18 variation was produced in an interval of 8 points, a minor change in comparison to the rest of
19 the cases, but visually appreciable in the resulting colour. In addition, this coordinate showed an
20 effect on initial solution concentration, since the green component was higher as the initial
21 solutions were more concentrated.

22 According to colorimetric results, it was possible to obtain a practically pure green shade when
23 spinel composition moved around $\Psi=0.5$ since no traces of neither blue nor yellow tones
24 appeared in the colour.
25
26
27
28
29
30
31
32
33
34
35
36
37
38
39
40
41
42
43
44
45
46
47
48
49
50
51
52
53
54
55
56
57
58
59
60
61
62
63
64
65

4 Conclusions

Molar concentration of the initial solution effect on the evolution of the solution combustion synthesis has been evaluated in the present study. In this case, SCS method allows synthesizing the Fd-3m spinel structures, characteristic of ceramic pigments with the solid solution composition (Co,Ni)Cr₂O₄. The presence of Ni²⁺ in the composition favours the appearance of a secondary phase with eskolaite structure, in a percentage lower than 5% wt. Certain influence of initial solution concentration was observed related to crystallinity parameters of the pigments.

The products of the most concentrated solutions showed a more ordered spinel network and a higher crystallite size than the diluted ones. Spinel lattice parameter was not influenced by the initial solution concentration. Nevertheless, it was directly affected by composition attending to Vegard's law, regardless the positive deviation observed from theoretical trend. Pigment morphology was modified depending on both composition and mixture concentration. The most Ni-rich spinel presented spherical grain shapes; however, samples with cobalt showed more angled grains, which were more similar to theoretical crystalline habit of a perfect spinel. For composition $\Psi=0.6$ and the highest concentration, grain sizes experienced a noticeable growth with well-defined grain borders and a compact structure.

Colouring power was intense in all cases and it was not highly affected by the concentration of initial solution. The colours generated in the selected glaze covered a broad palette of green shades. A progressive Co²⁺ content reduction provokes an increase in luminosity, a progressive reduction in green component and a change from a bluish hue towards a greenish one. In this study it has been possible to develop a green tone practically pure with the composition $\Psi=0.5$.

SCS method has been validated as an effective technique for spinel pigments synthesis since the products have high colouring power, and they are stable against variations in the molar concentration of the precursor's solution.

Acknowledgements

This work was supported by Universitat Jaume I (Project Nr. P11B2015-04).

Bibliography

- [1] A.S. Mukasyan, P. Dinka, Novel approaches to solution-combustion synthesis of nanomaterials, *Int. J. Self-Propagating High-Temp. Synth.* 16 (1) (2007) 23-35. doi: 10.3103/S1061386207010049
- [2] L.G. Gulsen, A. Kara, M. Blosi, D. Gardini, C. Zanelli, M. Dondi, Micronizing ceramic pigments for inkjet printing: Part I: Grindability and particle size distribution, *Ceram. Intern.* 41 (5) (2015) 6498-6506. doi: 10.1016/j.ceramint.2015.01.093
- [3] M. Dondi, M. Blosi, D. Gardini, C. Zanelli, P. Zannini, Ink technology for digital decoration of ceramic tiles: an overview, in: *Proceedings of the 13th World Congress on Ceramic Tile Quality, Qualicer 2014, Castellón (Spain), 17–18 February 2014*, pp. 1–14.
- [4] I. Hutchings, Ink-jet printing for the decoration of ceramic tiles: technology and opportunities, *Proceedings of the 12th World Congress on Ceramic Tile Quality, QUALICER, 2010, Castellón (Spain)*, 1–16.
- [5] C. Zanelli, G. L. Güngör, A. Kara, M. Blosi, D. Gardini, G. Guarini, M. Dondi, Micronizing ceramic pigments for inkjet printing: Part II. Effect on phase composition and color, *Ceram. Int.* 41 (2015) 6507–6517. doi: 10.1016/j.ceramint.2015.01.158
- [6] K.C. Patil, M.S. Hedge, T. Rattan, S.T. Aruna, *Chemistry of nanocrystalline oxide materials: Combustion synthesis, properties and applications*, World Scientific Publishing, Singapore, 2008.

- 1
2
3
4
5
6
7
8
9
10
11
12
13
14
15
16
17
18
19
20
21
22
23
24
25
26
27
28
29
30
31
32
33
34
35
36
37
38
39
40
41
42
43
44
45
46
47
48
49
50
51
52
53
54
55
56
57
58
59
60
61
62
63
64
65
- [7] A.C.F.M. Costa, A.M.D. Leite, H.S. Ferreira, R.H.G.A. Kiminami, S. Cava, L. Gama, Brown pigment of the nanopowder spinel ferrite prepared by combustion reaction, *J. Eur. Ceram. Soc.* 28 (2008) 2033-2037. doi:10.1016/j.jeurceramsoc.2007.12.039
- [8] S.S. Manoharan, K.C. Patil, Combustion synthesis of metal chromite powders, *J. Am. Ceram. Soc.* 75 (1992) 1012-1015. doi: 10.1111/j.1151-2916.1992.tb04177.x
- [9] S. Mestre, M.D. Palacios, P. Agut, Solution combustion synthesis of (Co,Fe)Cr₂O₄ pigments, *J. Eur. Ceram. Soc.* 32 (9) (2012) 1995–1999. doi:10.1016/j.jeurceramsoc.2011.11.044
- [10] S.T. Aruna, K.C. Patil, Synthesis and properties of nanosized titania, *J. Mater. Synth. Process.* 4 (3) (1996) 175-176.
- [11] K. C. Patil, S.T. Aruna, T. Mimani, Combustion synthesis: an update, *Curr. Opin. Solid State Mater. Sci.* 6 (2002) 507–512. doi:10.1016/S1359-0286(02)00123-7
- [12] K. C. Patil, S. T. Aruna, S. Ekambaram, Combustion synthesis, *Curr. Opin. Solid State Mater. Sci.* 2 (2) (1997) 158-165. doi doi:10.1016/S1359-0286(97)80060-5
- [13] S. T. Aruna, A. S. Mukasyan, Combustion synthesis and nanomaterials, *Curr. Opin. Solid State Mater. Sci.* 12 (2008) 44–50. doi:10.1016/j.cossms.2008.12.002
- [14] Color Pigments Manufacturers Association (CPMA), Classification and chemical descriptions of the complex inorganic color pigments, fourth ed., Alexandria (VA), 2013
- [15] J. Gilabert, M.D. Palacios, V. Sanz, S. Mestre, Characteristics reproducibility of (Fe,Co)(Cr,Al)₂O₄ pigments obtained by solution combustion synthesis, *Ceram. Int.* 42 (2016) 12880-12887. doi:10.1016/j.ceramint.2016.05.054
- [16] K.E. Sickafus, J.M. Wills, Structure of spinel, *J. Am. Ceram. Soc.* 82 (1999) 3279–3292. doi: 10.1111/j.1151-2916.1999.tb02241.x

[17] International Center for Diffraction Data (ICDD) PDF-4+ file, ICDD 04-004-8978

[18] J. Gilabert, M.D. Palacios, M.J. Orts, S. Mestre, Influencia de la temperatura en la síntesis de espinelas por combustión de una disolución, in: Proceedings of the LV Congreso de la Sociedad Española de Cerámica y Vidrio, SECV 2016, Seville (Spain), 5-7 October 2016, pp. 26-27

[19] G.Vandersnickt, W. Denolf, B. Vekemans, K. Janssens, μ -XRF/ μ -RS vs. SR μ -XRD for pigment identification in illuminated manuscripts, *Appl.Phys. A92* (2008) 59–68. doi: 10.1007/s00339-008-4447-

[20] P. A. Bland, G. Cressey, O. N. Menzies, Modal mineralogy of carbonaceous chondrites by X-ray diffraction and Mössbauer spectroscopy, *Meteoritics & Planetary Sci.* 39(1) (2004) 3–16. doi: 10.1111/j.1945-5100.2004.tb00046.x

[21] B. Fultz, J. Howe, *Transmission Electron Microscopy and Diffractometry of Materials*, fourth ed., Springer Berlin Heidelberg, 2013. doi: 10.1007/978-3-642-29761-8_1

[22] International Center for Diffraction Data (ICDD) PDF-4+ file, ICDD 04-014-1636

[23] International Center for Diffraction Data (ICDD) PDF-4+ file, ICDD 04-006-0279

[24] J. Shou-Yong, L.Z. Jin, L. Yong, Investigation on lattice constants of Mg-Al spinels, *J. Mater. Sci. Lett.* 19 (2000) 225-227. doi: 10.1023/A:1006710808718

[25] I.C. Nlebedim, J.E. Snyder, A.J. Moses and D.C. Jiles, Effect of deviation from stoichiometric composition on structural and magnetic properties of cobalt ferrite, $\text{Co}_x\text{Fe}_{3-x}\text{O}_4$ ($x = 0.2$ to 1.0), *J. Appl. Phys.* 111 (2012) 07D704. doi: 10.1063/1.3670982

[26] D.R. Lide (Ed), *CRC handbook of chemistry and physics*, 74th ed, CRC Press, Boca Raton, 1993.

1 [27] F. J. Torres, E. Ruiz de Sola, J. Alarcon, Effect of some additives on the development of
2 spinel-based glass-ceramic glazes for floor-tiles, *J. of Non-Cryst. Solids* 351 (2005) 2453–2461.
3
4 doi: 10.1016/j.jnoncrysol.2005.06.027
5

6
7 [28] T. Maiyalagan, K. R. Chemelewski, A. Manthiram, Role of the morphology and surface
8 planes on the catalytic activity of spinel $\text{LiMn}_{1.5}\text{Ni}_{0.5}\text{O}_4$ for oxygen evolution reaction, *ACS*
9 *Catal.* 4 (2014) 421–425. doi: 10.1021/cs400981d
10
11

12 [29] S.A. Eliziário, J.M. de Andrade, S.J.G. Lima, C.A. Paskocimas, L.E.B. Soledade, P.
13 Hammer, E. Longo, A.G. Souza, I.M.G. Santos, Black and green pigments based on chromium–
14 cobalt spinels, *Mater. Chem. Phys.* 129 (1-2) (2011) 619–624. doi:
15
16 10.1016/j.matchemphys.2011.05.001
17
18
19
20
21
22
23
24

25 [30] M. Gaudon, L.C. Robertson, E. Lataste, M. Duttine, M. Ménétrier, A. Demourgues, Cobalt
26 and nickel aluminate spinels: Blue and cyan pigments, *Ceram. Int.* 40 (4) (2014) 5201–5207.
27
28
29
30
31
32
33
34
35
36
37
38
39
40
41
42
43
44
45
46
47
48
49
50
51
52
53
54
55
56
57
58
59
60
61
62
63
64
65

66 [31] J. Alarcón, P. Escribano, R.M^a. Marín, Co(II) based ceramic pigments, *Br. Ceram. Trans. J.*
67 84 (1985) 170-172

Figure captions

Figure 1 EDX chemical analysis of SCS spinels comparing experimental and theoretical values

Figure 2 XRD phase identification for all composition range of (Co,Ni)Cr₂O₄ samples at 1.2M concentration (○ spinel, ● eskolaite)

Figure 3 Mass percentage of secondary eskolaite phase in pigments versus composition and initial solution concentration

Figure 4 Evolution of the XRD main peak of the pigments versus Ψ and concentration of initial solution

Figure 5 Evolution of crystallite size depending on parameter Ψ

Figure 6 Comparison of cell parameters of the spinel with the prediction of Vegard's law, based on the ICCD data from the spinels CoCr₂O₄ ($\Psi=0.0$) and NiCr₂O₄ ($\Psi=1.0$)

Figure 7 Micrographies obtained by SEM of selected pigments

Figure 8 BJH curves showing pore size distribution of selected samples

Figure 9 Reflectance curves of the glazes that contain the synthesized pigments (2.4M samples), indicating the bands related to electron transitions of Ni²⁺, Co²⁺ and Cr³⁺ ions located in spinel crystals

Figure 10 Evolution of the glaze's chromatic coordinates versus studied parameters of incorporated pigments (Ψ and initial solution concentration): a) L*, b) b* and c) a* coordinates

Tables and table captions

Table 1 Composition of initial solutions

Ref.	Ψ	Urea (g)	Co(NO ₃) ₂ ·6H ₂ O (g)	Ni(NO ₃) ₂ ·6H ₂ O (g)	Cr(NO ₃) ₃ 9H ₂ O (g)	H ₂ O (mL)
S1	0.0	24.0	17.46	0.00	48.0	25 / 50 /100
S2	0.2	24.0	13.96	3.49	48.0	25 / 50 /100
S3	0.4	24.0	10.47	6.98	48.0	25 / 50 /100
S4	0.6	20.0	5.82	8.72	40.0	21 / 42 /84
S5	0.8	16.8	2.44	9.77	33.6	18 / 35 /70
S6	1.0	16.8	0.00	12.21	33.6	18 / 35 /70

Table 2 Specific surface area values (m²/g) for selected samples

Composition	Initial solution concentration	
	Low	High
$\Psi = 0.0$	11.5	10.6
$\Psi = 0.6$	15.4	12.3
$\Psi = 1.0$	16.2	11.3

Figure 1

[Click here to download high resolution image](#)

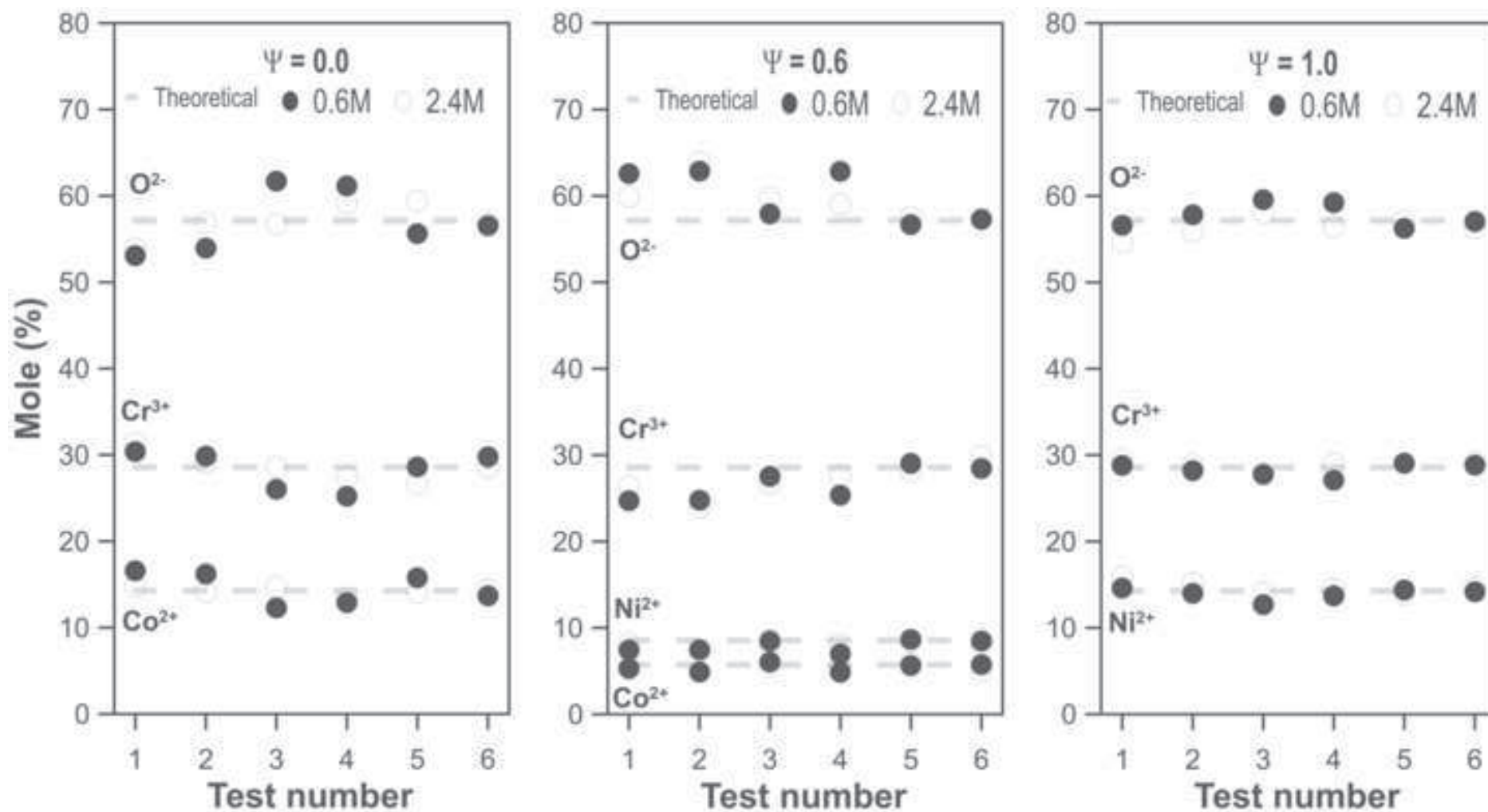


Figure 2
[Click here to download high resolution image](#)

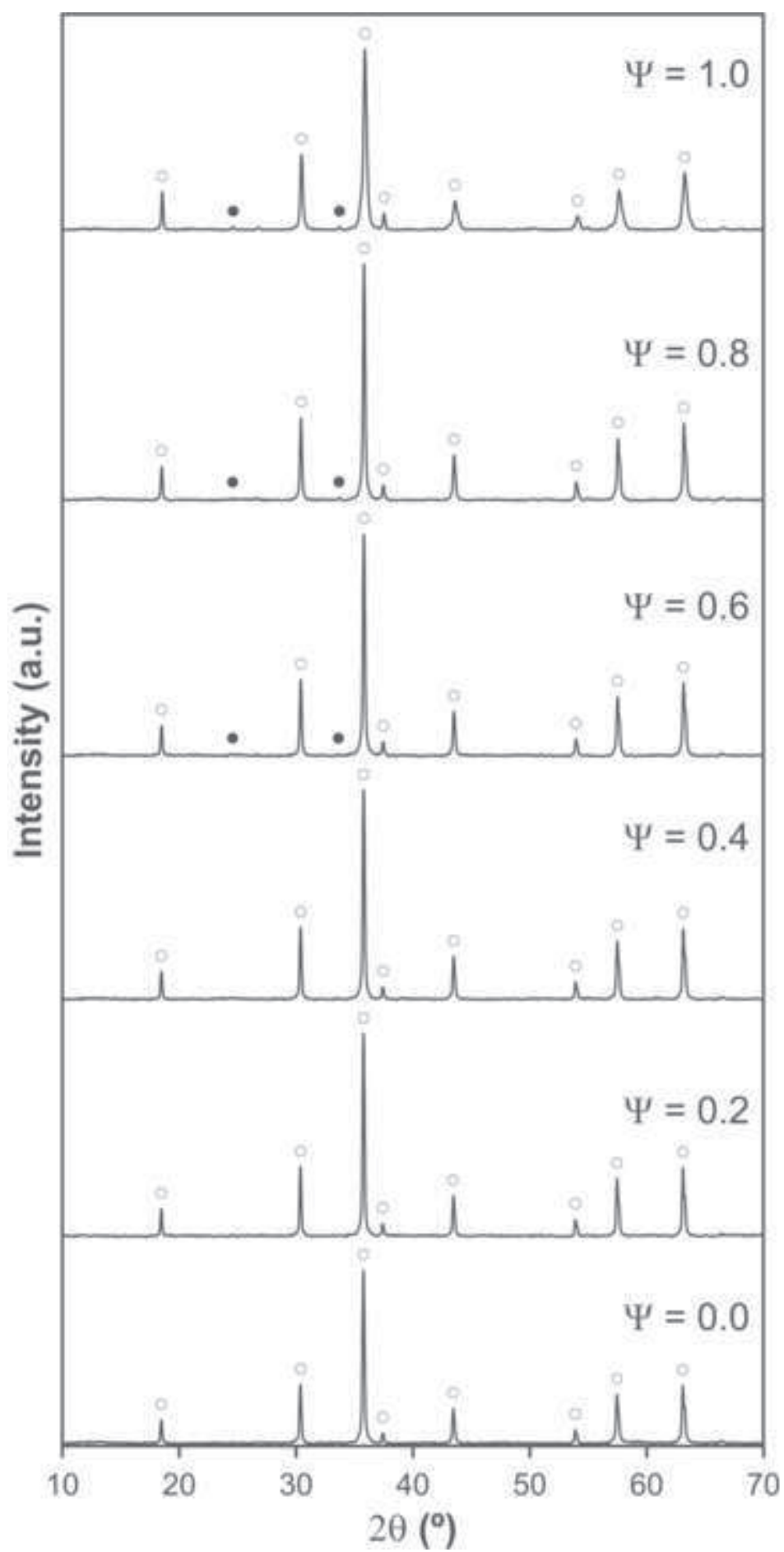


Figure 3

[Click here to download high resolution image](#)

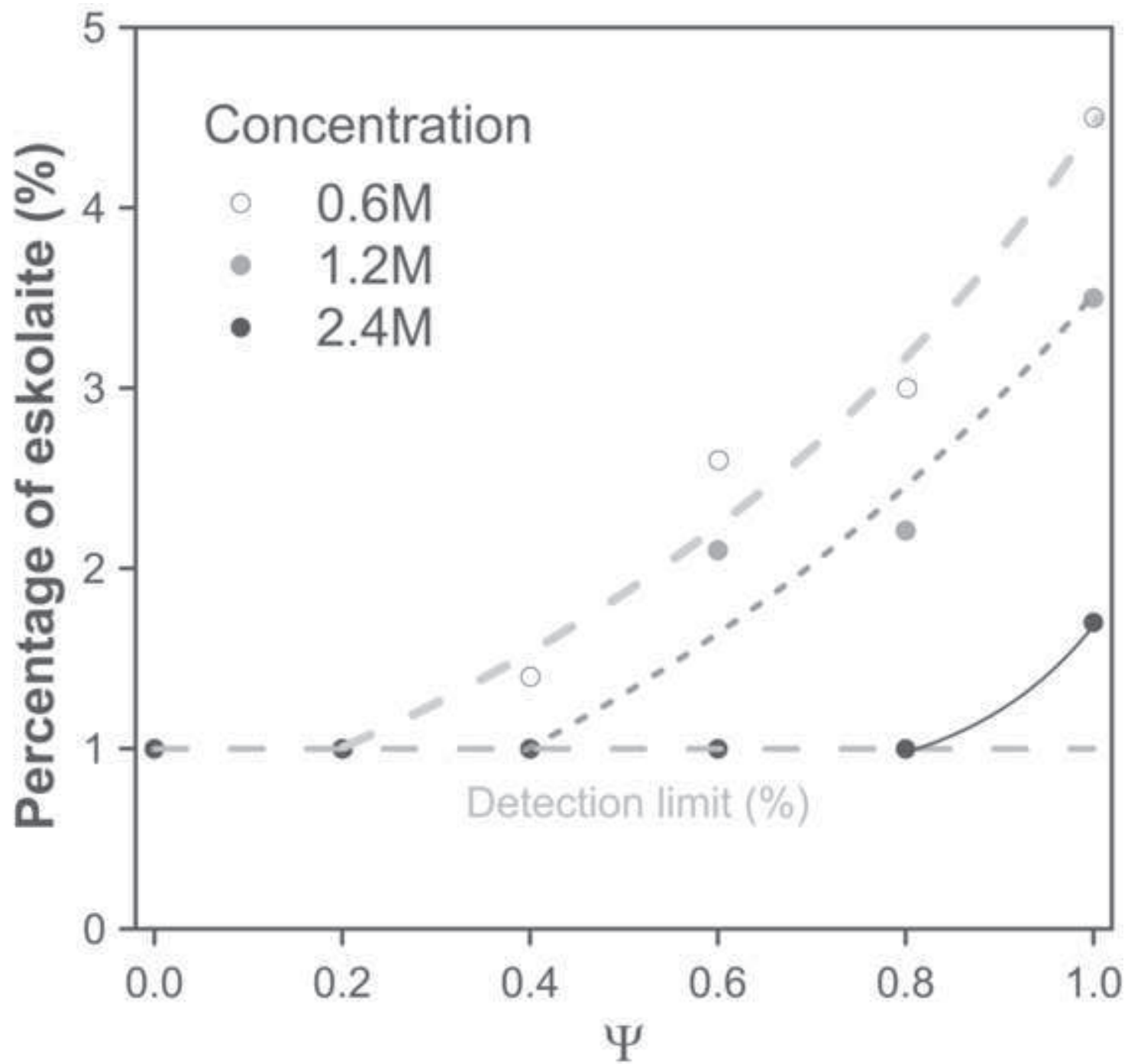


Figure 4
[Click here to download high resolution image](#)

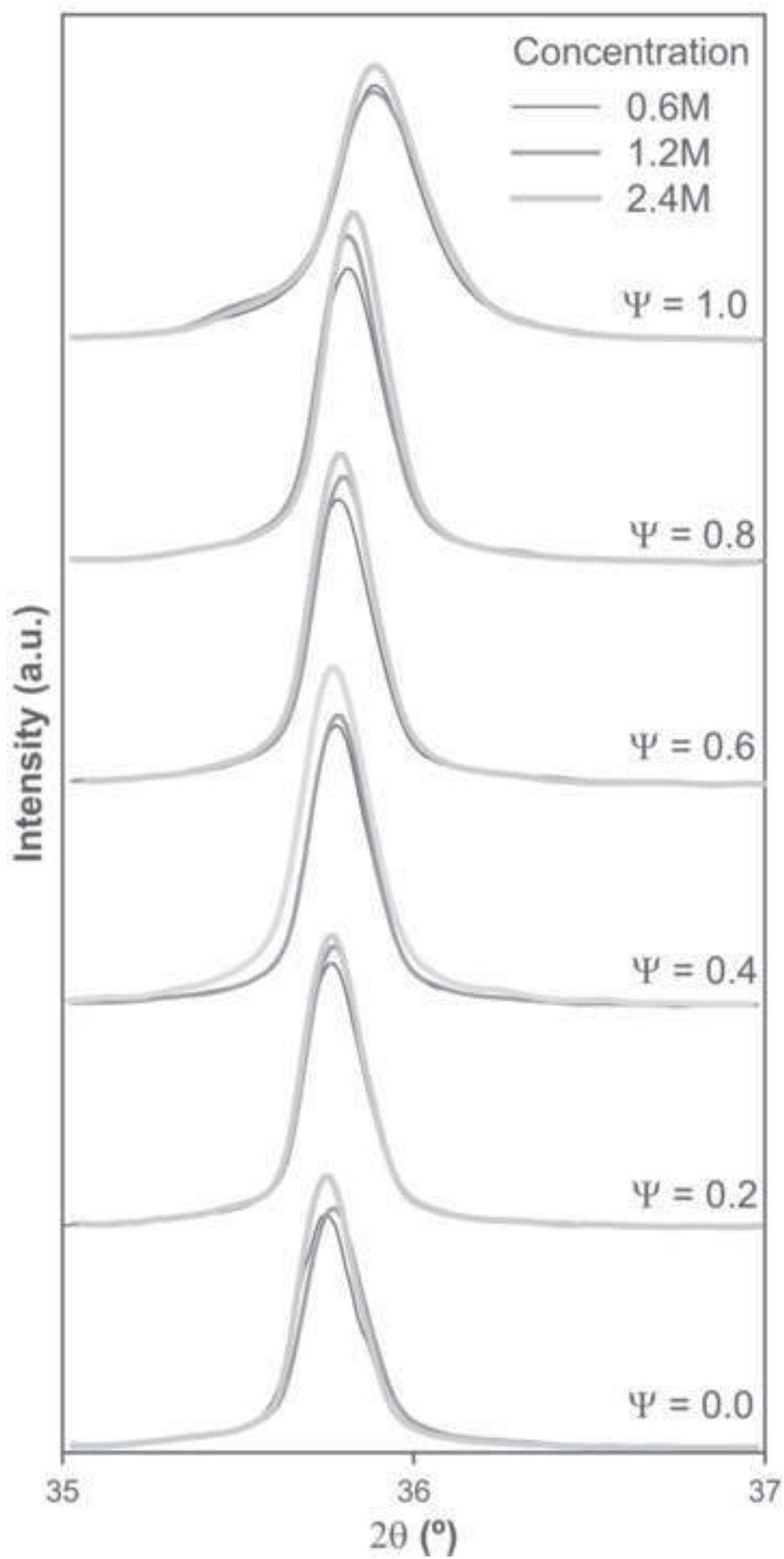


Figure 5

[Click here to download high resolution image](#)

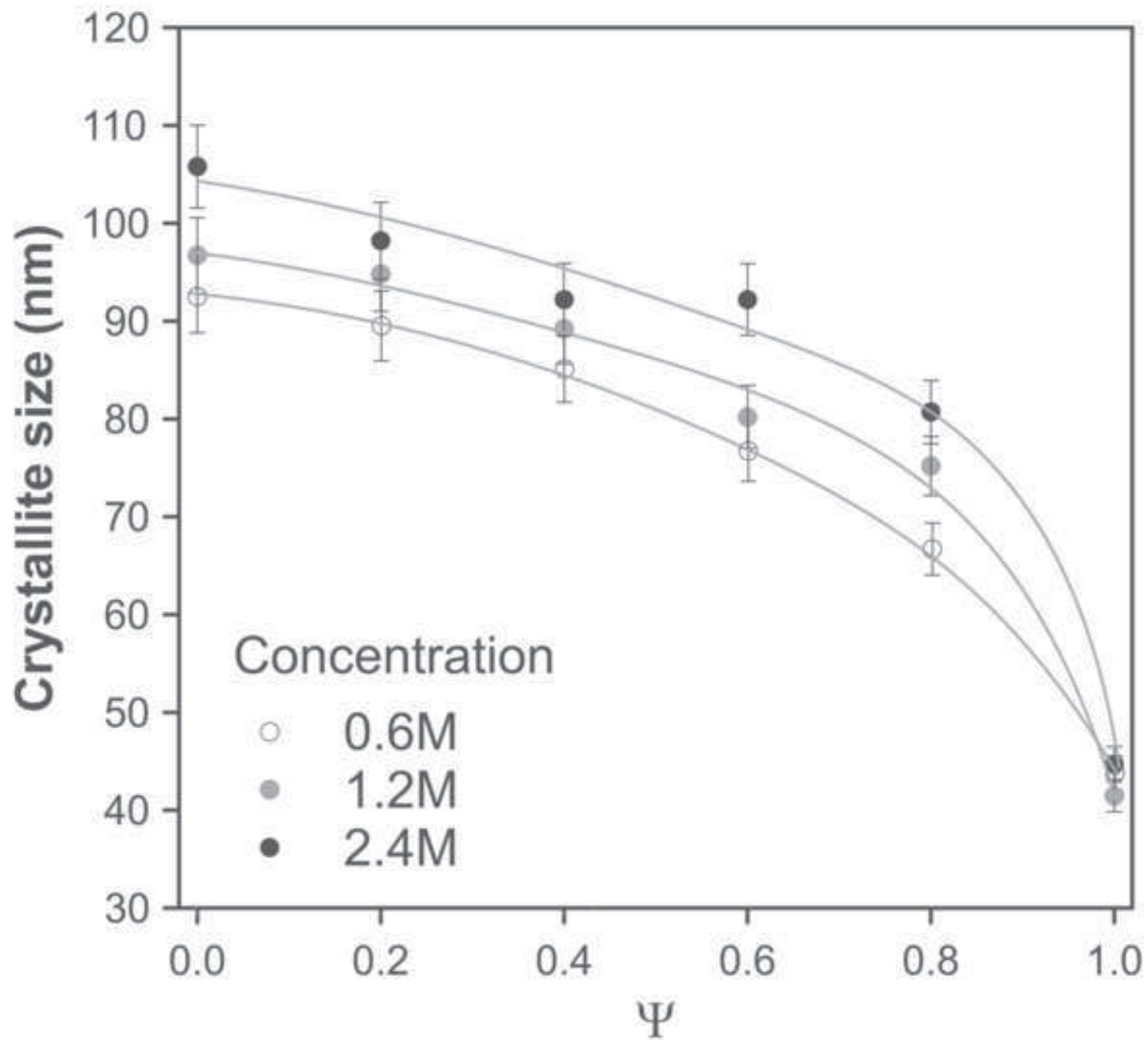


Figure 6

[Click here to download high resolution image](#)

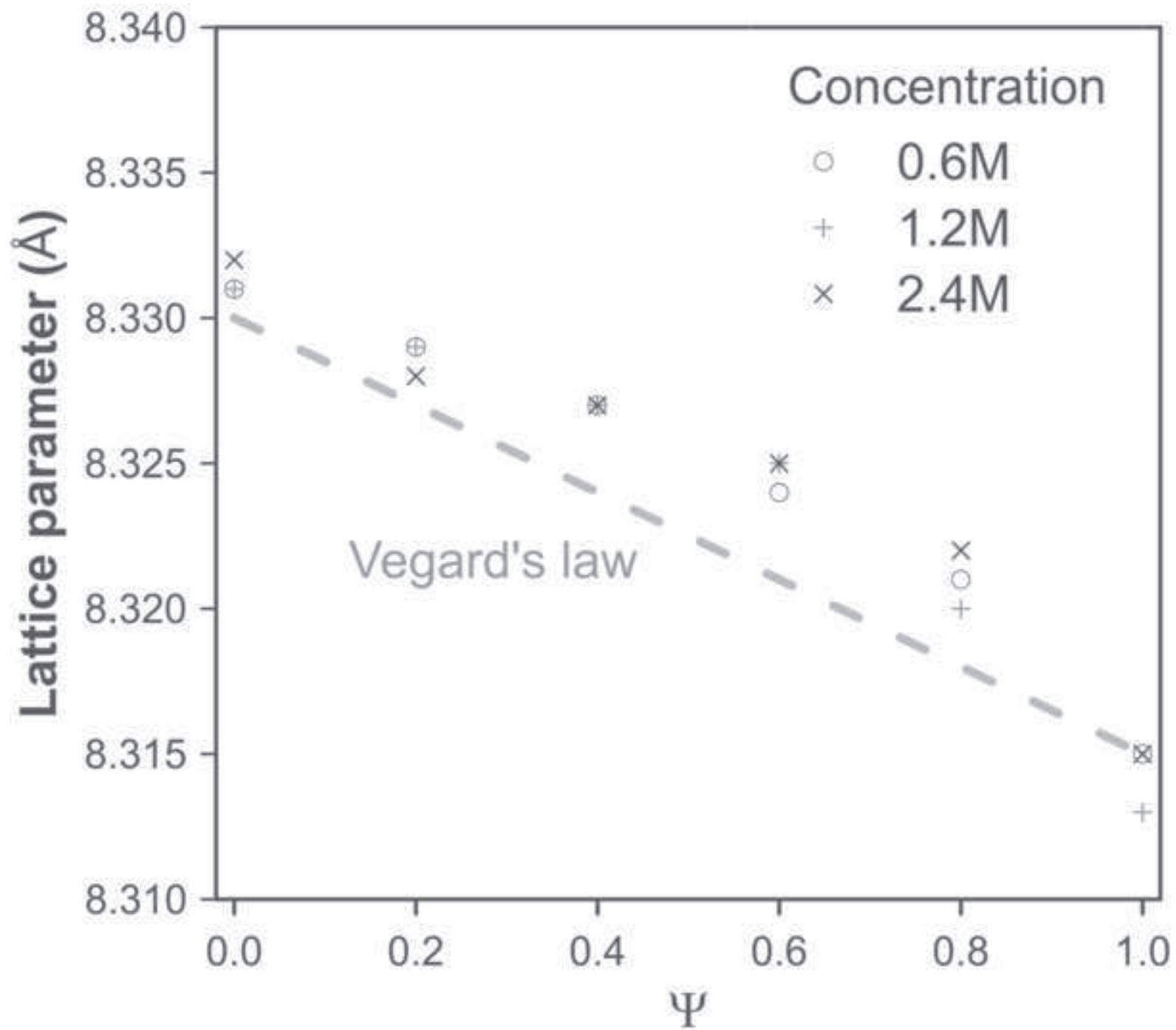


Figure 7
[Click here to download high resolution image](#)

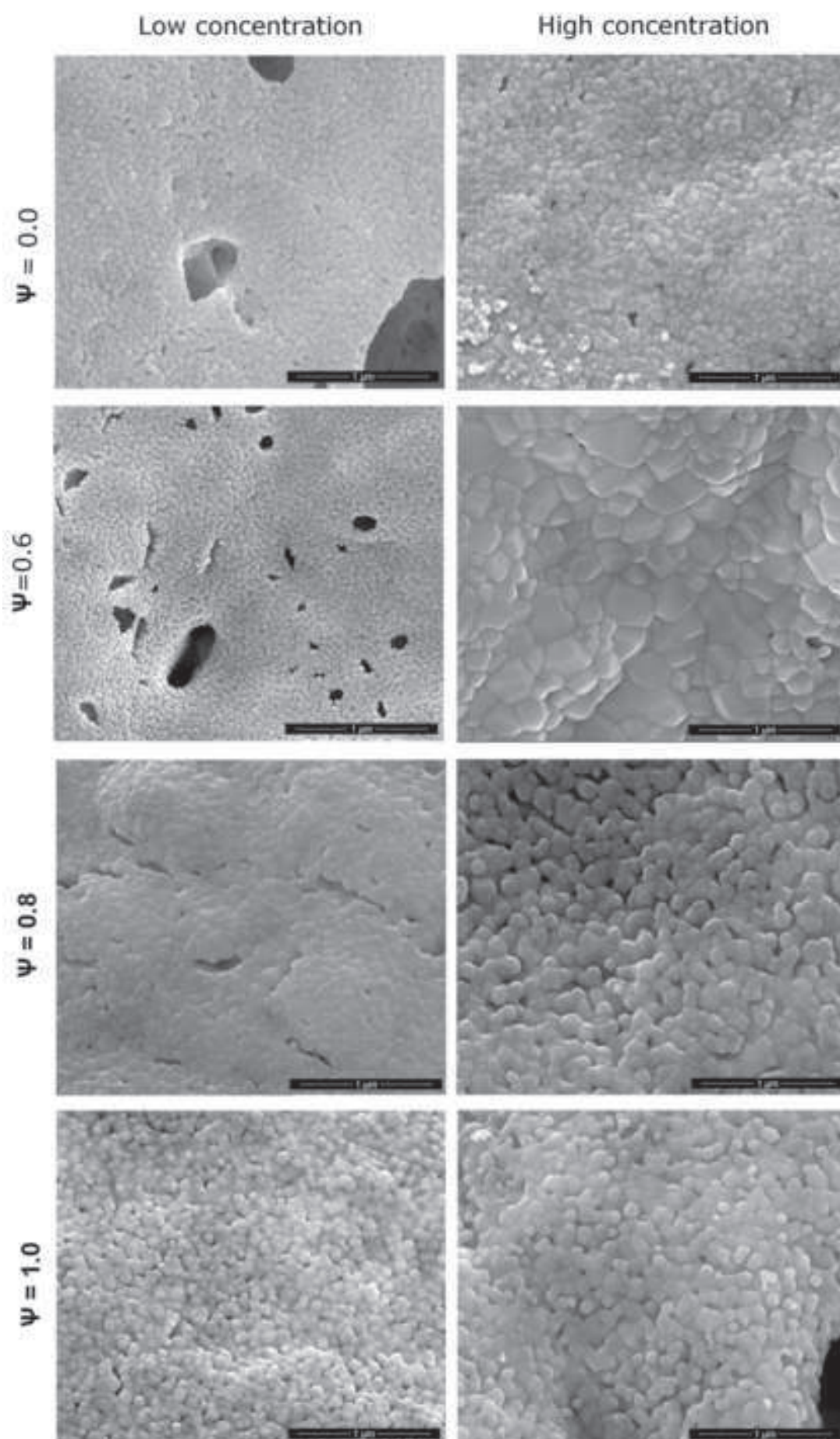


Figure 8

[Click here to download high resolution image](#)

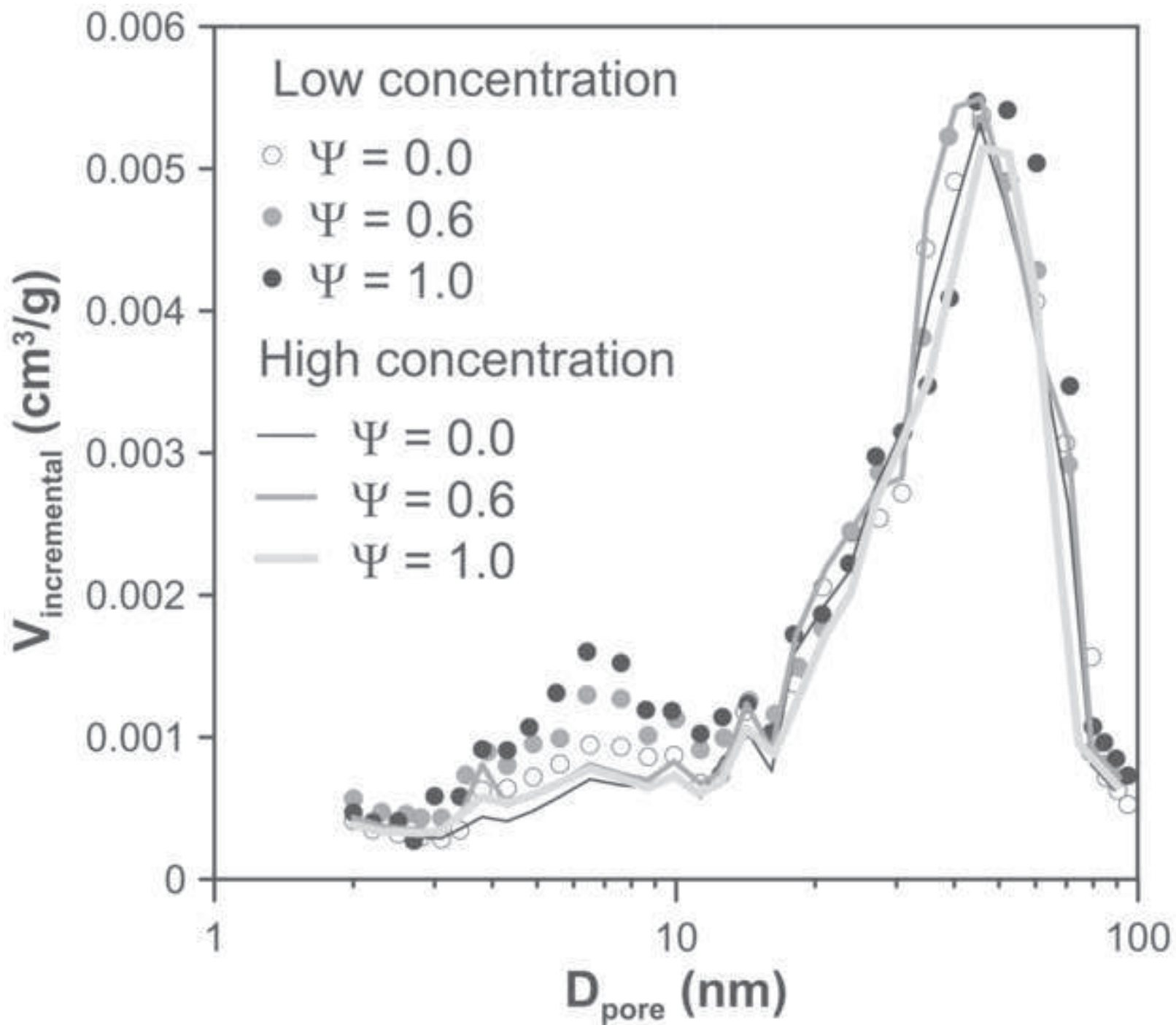


Figure 9

[Click here to download high resolution image](#)

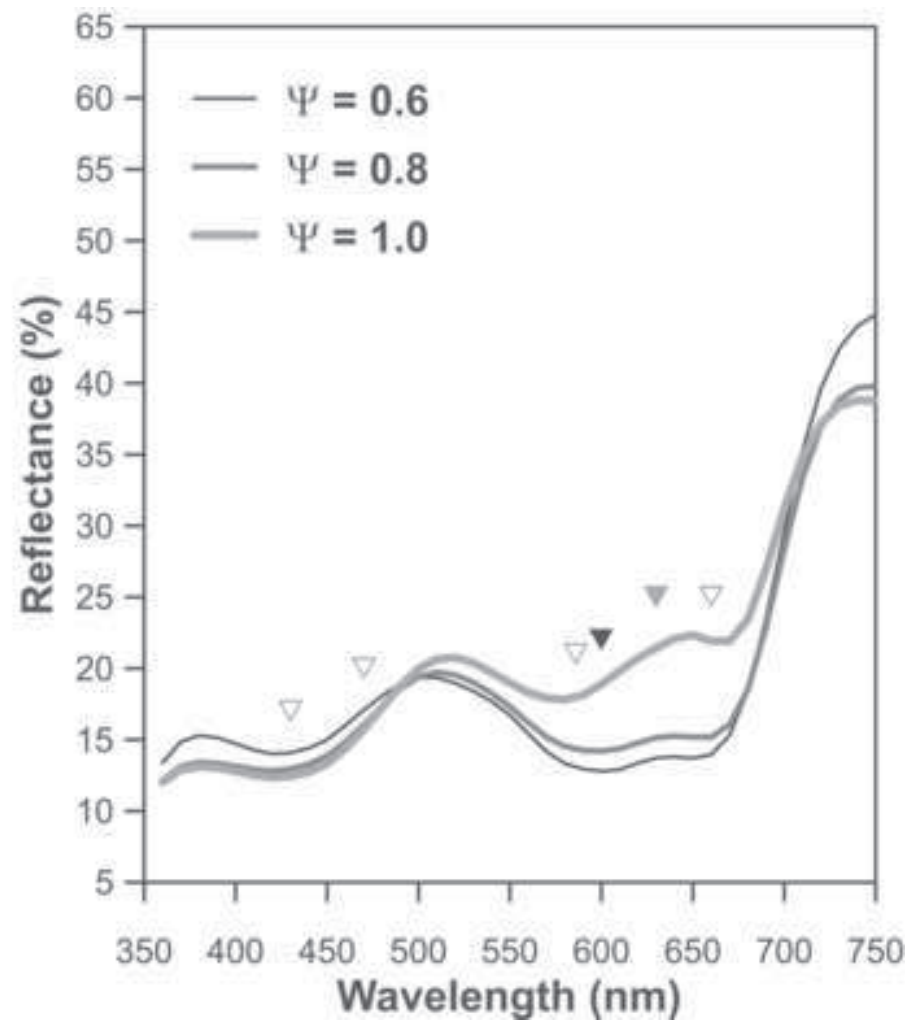
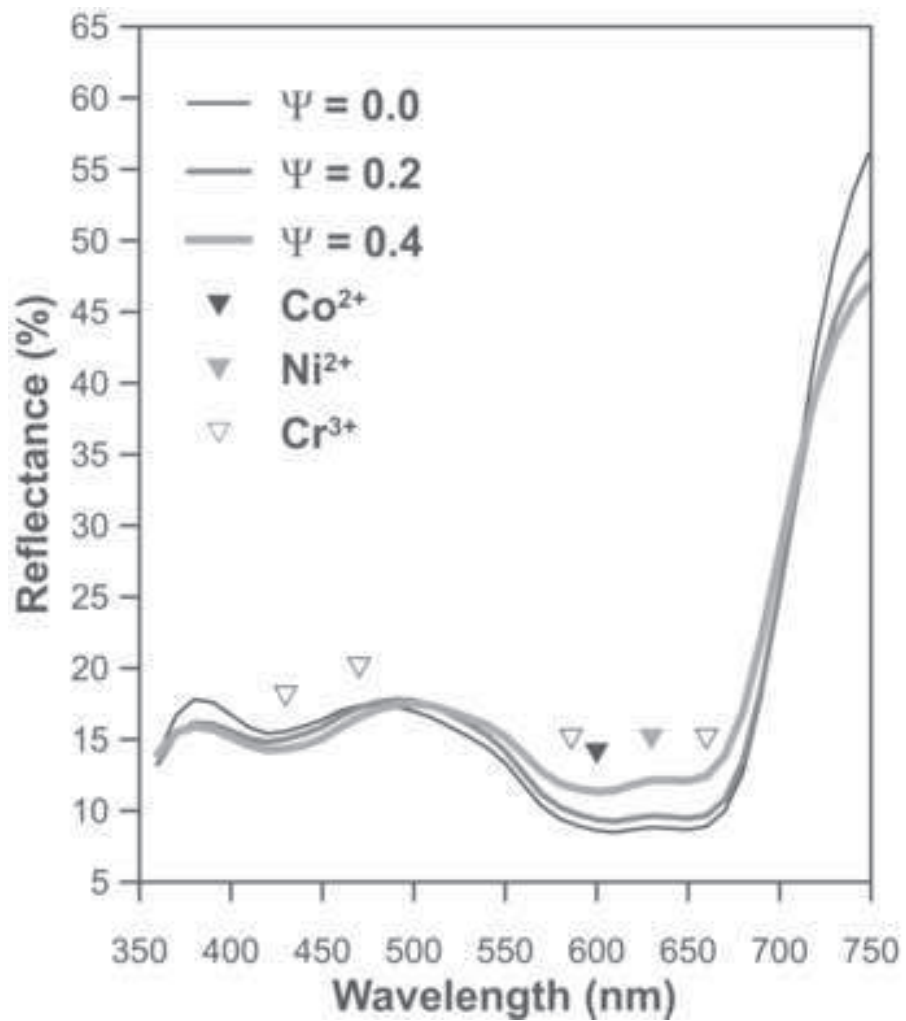


Figure 10
[Click here to download high resolution image](#)

